MAGNETIC PARTICLE MOTIONS WITHIN LIVING CELLS

Measurement of Cytoplasmic Viscosity and Motile Activity

P. A. VALBERG AND H. A. FELDMAN
Department of Environmental Science and Physiology, Harvard School of Public Health, Boston, Massachusetts 02115

ABSTRACT Submicrometer magnetic particles, ingested by cells and monitored via the magnetic fields they generate, provide an alternative to optical microscopy for probing movement and viscosity of living cytoplasm, and can be used for cells both in vitro and in vivo. We present methods for preparing lung macrophages tagged with magnetic particles for magnetometric study. Interpretation of the data involves fitting experimental remanent-field decay curves to nonlinear mechanistic models of intracellular particle motion. The model parameters are sensitive to mobility and apparent cytoplasmic viscosity experienced by particle-containing organelles. We present results of parameter estimation for intracellular particle behavior both within control cells and after (*a*) variable magnetization duration, (*b*) incubation with cytochalasin D, and (*c*) particle twisting by external fields. Magnetometric analysis showed cytoplasmic elasticity, dose-dependent motion inhibition by cytochalasin D, and a shear-thinning apparent viscosity.

INTRODUCTION

Cytoplasmic Motility

Measurements of the physical properties of living cytoplasm can contribute to a more complete understanding of cellular function. As reviewed by Porter (1984), structure of the cytoplasmic matrix has been the subject of intense study and debate for many years, and advances in molecular biology have provided new insights into how the formed elements of cytoplasm interact in diverse cellular processes. The cytomatrix has emerged as a regulating factor in cytoplasmic organization, cellular and intracellular motions, and cell shape. However, techniques have not been available to detect how modifications of the cytomatrix in living cells alter the physical, rheological properties of the cytoplasm.

Magnetic Particles as a Probe

One experimental approach for quantifying cytoplasmic motility and rheology involves magnetometrically detecting the movements of magnetic particles that have been phagocytized by cells. The motion of magnetic particles within human subjects was first recognized in magnetometer data by Cohen (1973), who called the remanent-field decay due to this motion "relaxation." Magnetometry has been applied to detect particle motion both in animals (Gehr et al., 1983; Brain et al., 1984) and in isolated cells (Valberg, 1984; Gehr et al., 1985; Nemoto et al., 1985). Magnetic particles offer an alternative to optical observation via the light microscope as a means of monitoring spontaneous cytoplasmic motile activity. Intracellular particle motion results from the balance of cellular forces applied against the viscous drag offered by the cytoplasmic environment. The observation of changes in relaxation per se cannot determine which of these two factors has been affected. However, external fields can be used to apply a known torque to aligned particles, and the rate of particle reorientation is a measure of intracellular viscosity. We present results of magnetometric measurements made on isolated lung macrophages and show how such data can be used to estimate intracellular motions and cytoplasmic viscosity.

Data Interpretation

In previous investigations, relaxation curves measured in situ for hamsters, rabbits, and humans have been summarized with several ad hoc parameters estimated from small sections of the curve. The initial relaxation rate (dB_r/dt at $t \approx 0$) was estimated by regression during the first 60 s of data, assuming the exponential decay; initial field strength (B_{r0}) was obtained from extrapolation of the regression line; relaxation half-time [$B_r(T_{1/2}) = \frac{1}{2}B_{r0}$] was the time point at which remanent field strength was half its initial magnitude, B_{r0} (Gehr et al., 1983; Brain et al., 1984; Cohen et al., 1984). An improved procedure is to identify mathematical equations describing the complete time course of relaxation (Valberg and Butler, 1987). Magnetometric data can then be fitted to the equation using

Address correspondence to Peter A. Valberg, Department of Environmental Science and Physiology, Harvard School of Public Health, 665 Huntington Avenue, Boston, MA 02115.

least-squares procedures for nonlinear parameter estimation. In this way, not only can we find parameters that respond in a precise way to experimental manipulations, but we can also evaluate mechanistic particle-motion theories expressed in terms of such equations.

METHODS

Cell Preparation with Magnetic Iron Oxide

Iron oxide particles have been used both for particle phagocytosis studies and for studies of aerosol deposition and clearance in lungs (Gibb and Morrow, 1962; Sorokin and Brain, 1975; Kavet et al., 1978; Grant et al., 1979). Iron oxide is visible in cells with the light microscope due to its pigmentation and with the electron microscope due to its electron opacity. Magnetic iron oxide can be quantified down to microgram quantities with fluxgate or SQUID (superconducting quantum interference device) magnetometers (Cohen, 1978).

Lung macrophages were magnetically tagged by having hamsters breathe a submicrometric aerosol of γ-Fe_2O_3 (gamma hematite) generated de novo by controlled combustion of $Fe(CO)_5$ vapors (Valberg and Brain, 1979). Gamma hematite is familiar as the brown particulate bonded into magnetic recording tapes. During animal inhalation exposure, the generator was connected to a 40-liter Lucite chamber where 1–8 Syrian golden hamsters (~120 g bw) breathed the γ-Fe_2O_3 aerosol (mass median aerodynamic diameter $\approx$ 0.7 μm; mass concentration $\approx$ 300 μg/liter) for 1–3 h. Hamster minute ventilation is ~60 ml, and each hour of exposure produced ~180 μg of lung-deposited particles. By 24 h after aerosol inhalation, particles deposited on airways have been removed by mucociliary action, and almost all particles landing on nonciliated lung surfaces have been phagocytized by lung macrophages (Sorokin and Brain, 1975).

Lung macrophages were harvested by multiple saline lung lavages (Brain and Frank, 1968). Hamsters were anesthetized by an intraperitoneal injection of pentobarbital sodium (600 mg/kg body wt). The lungs were cannulated with polyethylene tubing, connected to a syringe, and "washed" 12 times by repetitively instilling and withdrawing 3-ml aliquots of isotonic saline. The absence of divalent cations in the isotonic saline and gentle massage of the chest promote detachment of macrophages from lung surfaces. Lung lavage 1 d after inhalation exposure recovered 6–8 $\times$ 10^6 macrophages, which contained ~50% of the lung-retained magnetic material. Average particle content as a percent of cell volume averaged 0.5–1.5%.

The harvested cells were separated from the lavage fluid and any remaining free particles by centrifugation. The settling velocity in a fluid can be derived from the balance of gravitational (or centrifugal) force against viscous resistance:

$$(\rho - \rho_{\text{fluid}}) \frac{\pi g d^3}{6} = 3 \pi \eta d v_s, \quad (1)$$

where ρ is density, g is acceleration (gravity or centrifugal), d is particle or cell diameter, and η is fluid viscosity. The settling velocity, v_s, is given by

$$v_s = (\rho - \rho_{\text{fluid}}) \frac{g d^2}{18 \eta}. \quad (2)$$

Macrophages have an average diameter of 11 μm and range in specific gravity from 1.04 to 1.10 (Chandler et al., 1986), with ρ increasing to 1.06–1.12 for macrophages that have ingested 0.5% of their cytoplasmic volume in iron oxide particles (specific gravity 4.6). The size range of iron oxide particles can be calculated from the particle aerodynamic size distribution (Valberg and Brain, 1979). The mass median equivalent spherical diameter is 0.43 μm, with 95% of the particle mass in the diameter range 0.16–0.60 μm. Centrifugation at 100$\times$ gravity (for 5 min) causes the least-dense cells to settle a distance of 17 cm, but the mass median particle falls only 1.4 cm. Thus, a single centrifugation in 10-cm-long tubes would collect all the cells, but only ~14% of any free particles that remain.

The cell pellet was redispersed in RPMI 1640 culture medium with 0.2% bovine serum albumin (BSA) and 25 mM Hepes buffer (pH 7.4 at 37°C), and cells were counted and sized with a Coulter counter (Coulter Electronics, Hialeah, FL). Macrophages represented >95% of the recovered cells, and viability by Trypan blue dye exclusion was 85–94%. The particle content of macrophages was ~30 μg γ-Fe_2O_3 per 10^6 cells, as measured by magnetometry. Macrophage aliquots (~10^5 cells) in the culture medium were placed into glass or plastic 1.5-ml vials (vial 228778, Wheaton Industries, Millville, NJ; or tissue culture well 6350, Dynatech Laboratories, Inc., Alexandria, VA). Incubation for 1–2 h at 37°C in an atmosphere of 95% air and 5% CO_2 resulted in 80–90% of the macrophages attaching firmly to vial surfaces; the adherent cells were ready for relaxation measurements. Cells can also be prevented from floating freely by centrifuging them into a pellet, or by trapping them in soft agar gels (Reppun et al., 1979). Such preparations hold the cells immobile and permit detection of intracellular motions of magnetic particles, while allowing oxygenation and nutrition to continue.

Lavaged lung macrophages exhibit considerable heterogeneity in particle content (Sorokin and Brain, 1975), and this heterogeneity may be related to macrophage functional status (Valberg and Mariak, 1984). A cell population that has ingested magnetic particles can be fractionated according to magnetic particle content. If macrophages containing magnetic material are placed in nonuniform magnetic field, the cells experience a translational force in the direction of increasing magnetic field intensity. The size of this force increases with the quantity of magnetic material present. An electromagnet can be used to generate a magnetic-field gradient of variable intensity, and cells in suspension can be passed into this region via tubing; cells will be pulled adjacent to the magnet depending upon their particle content (Kronick, 1980). The portion of the cells retained adjacent to the magnet are released by turning off the current (and demagnetizing) and are collected as a single fraction. Repeating this procedure with successively increasing magnetic-field gradients separates the cell population according to quantity of magnetic material per cell.

Relaxation Curve Measurement

The magnetometry apparatus maintained the cell vial and its contents at a temperature of 37°C and an atmosphere of 5% CO_2 in air while in the magnetically shielded sensing volume. Fluxgate detectors monitored the weak remanent magnetic field from the cells, as described in the preceding paper (Valberg and Butler, 1987). The magnetic directions of the intracellular particles were aligned either outside the measurement apparatus by application of a permanent magnet or while within the apparatus by a transient current pulse in Helmholtz coils that surround the cell vial. The magnetization of each particle is permanent, but independent and varying rotation of many intracellular particles gradually randomizes the initially parallel magnetization directions, causing the collective remanent field from the particles to decrease. This "relaxation" was digitized every 0.2 s and recorded on magnetic disk (4110T electronic recorder, Bascom-Turner Instruments, Norwood, MA).

Microscopy

For video microscopy and photomicrography, macrophages adherent to glass coverslips (37°C, 1 h) were inverted on a drop of culture medium and sealed on a glass slide with Vaseline. Cells and their internalized particles were placed on the warm (37°C) stage of a Zeiss Photoscope III and were viewed under brightfield, phase-contrast, or Normarski differential-interference contrast (DIC) optics. Lavaged, particle-containing macrophages were also prepared for examination by electron microscopy. Cells were pelleted, fixed (2.5% glutaraldehyde in 0.16 M potassium

phosphate buffer for 1 h at *RT*, postfixed with 1% OsO_4 in 0.1 M sodium cacodylate), dehydrated in graded ethanols and propylene oxide, and embedded in Epox. Thin sections were cut using a diamond knife in a MT6000 microtome (Sorvall Instruments Div., Newton, CT). The sections were stained with uranyl acetate and lead citrate and examined in a Philips 300 transmission electron microscope.

Magnetization Duration Experiments

Most human and animal magnetometric studies magnetize particles within the body by a high magnetic field applied for the order of minutes (Cohen et al., 1984; Cohen and Nemoto, 1984). Our morphological evidence showed that magnetization of cells with a permanent magnet caused particles to link up in chains (cf. Fig. 2), and there was evidence of intermediate-filament reorganization (Valberg and Albertini, 1985). We sought to examine how the magnetization regimen affected the relaxation process. Cells from four animals were divided into four aliquots (16 vials total), and each vial was magnetized four separate ways. The sequence was, first, pulse magnetization (~10-μs pulse), then 12-s magnetization, then 120-s magnetization, and finally 1,200-s magnetization duration. A relaxation curve was measured after each magnetization.

Cytochalasin Experiments

Cytochalasins are natural mold metabolites that inhibit cell functions requiring cytoplasmic movement. Cytochalasin D (cytD), from the mold *Metarrhizium anisopliae*, interferes with the organization of actin filaments by capping the fast-growing end (MacLean-Fletcher and Pollard, 1980*a*), and has been shown to inhibit phagocytosis of 2-μm latex beads by alveolar macrophages (Parod and Brain, 1986). We sought to characterize its effect on relaxation. Lung macrophages from six separate animals were divided into eight aliquots that were incubated with different concentrations of cytD dissolved in a dimethylsulfoxide (DMSO) vehicle. The cytD concentrations ranged from 0 (DMSO alone) to 10 μM. Relaxation curves were measured immediately before cytD addition and at 15 min after addition.

Particle "Twisting" Experiments: Procedure

The apparent viscosity of the magnetic-particle environment was determined by measuring the response of the particles to a magnetically driven reorientation. Intracellular particles were initially magnetized horizontally, perpendicular to the cell vial axis, as usual. A weak magnetic field ($H_a \approx 2.5$ mT) was then applied along the axis of the vial, at right angles to the original magnetizing field. H_a did not change the magnetic state of the particles but did exert a torque driving them to physically rotate their magnetic axes parallel to the vial axis. As the intracellular particles were twisted toward this vertically applied "twisting" magnetic field, the vector component of the remanent magnetic field sensed by the fluxgate probes [$B_{r,twist}(t)$] was reduced. $B_{r,twist}(t)$ decreased with time in a way that is related to both the strength of the twisting field (H_a) and the apparent viscosity (η) as was derived in the preceding paper (Eq. 11 in Valberg and Butler, 1987). $B_{r,twist}(t)$ is independent of particle diameter; the apparent viscosity (η) can be estimated from the experimental measurements of $B_{r,twist}(t)$.

Particle "Twisting" Experiments: Theory

To interpret the contributions of particle twisting and spontaneous cytoplasmic movements to the overall decay curve, we consider the particle motions in a coordinate system where the original magnetic alignment occurs along the x-axis and the twisting field is applied along the z-axis. The result of random cytoplasmic impulses is to slowly spread out the moment distribution, which initially is peaked about the x-axis; the net moment remains parallel to the x-axis but decreases in magnitude. This produces the remanent-field decay data due to relaxation alone, $B_{r,notwist}(t)$. Imposition of the twisting field causes particle magnetic moments to rotate at a rate that depends on the balance between magnetic torque and viscous retardation. The distribution of particle angles rotates toward the z-axis, as if pivoted about the y-axis. If we assume that the application of the particle twisting field does not modify normal cytosolic relaxation processes, the curve resulting from twisting and relaxation occurring simultaneously, $B_{r,twist}(t)$, can be thought of as the result of viewing relaxation alone [$B_{r,notwist}(t)$] from a coordinate system rotating at $\theta(t)$. That is,

$$B_{r,twist}(t) = B_{r,notwist}(t) \sin \theta(t), \quad \text{where } \theta(0) = \pi/2. \tag{3}$$

The rotation of moments by a twisting field was discussed in the preceding paper (Valberg and Butler, 1987), and the rate of rotation is given by Eq. 7 in that paper:

$$\frac{\partial \theta}{\partial t} = -\frac{\sin \theta}{\tau_{lo}}, \quad \text{where } \tau_{lo} = \left(\frac{\kappa \eta}{\mu_o M_r H_a}\right).$$

Rewriting this, and explicitly allowing for the fact that η can have a shear-rate dependence, we have

$$\eta(\dot{\theta}) = -k \frac{\sin \theta}{\dot{\theta}}, \quad \text{where } k = \frac{\mu_o M_r H_a}{\kappa}. \tag{4}$$

Data Analysis

Experimental data consisted of points [t, $B_r(t)$] collected at frequent intervals, where $B_r(t)$ denotes the remanent field at time t. We used nonlinear least-squares procedures (Jennrich and Ralston, 1979) to fit the data with one of the following theoretical models for $B_r(t)$, obtaining estimates and standard errors for the various kinetic parameters. (*a*) Brownian rotation or single exponential model (Nemoto, 1982; Valberg and Butler, 1987)

$$B_r(t) = B_{r0} e^{-\gamma t}. \tag{5}$$

(*b*) Double-exponential model of Brownian motion for two particle populations:

$$B_r(t) = B_{r0} [f e^{-\gamma_1 t} + (1-f) e^{-\gamma_2 t}]. \tag{6}$$

(*c*) Rotational diffusion of rods experiencing entanglement constraints (Doi and Edwards, 1978)

$$B_r(t) = B_{r0} e^{-\sqrt{\lambda t} - \gamma t}. \tag{7}$$

(*d*) Linear-track pulling of vesicles anchored at one end (Valberg and Butler, 1987):

$$B_r(t) = B_{r0} [1 + (\alpha t)^\beta]^{-1/2}. \tag{8}$$

(*e*) Simultaneous linear-track and Brownian rotational motion operating independently:

$$B_r(t) = B_{r0} e^{-\gamma t} [1 + (\alpha t)^\beta]^{-1/2}. \tag{9}$$

For data from twisting of intracellular magnetic particles by an external field, at each time point t we constructed the ratio

$$\frac{B_{r,twist}(t)}{B_{r,notwist}(t)} = \sin \theta(t). \tag{10}$$

An empirical curve was fitted to $\theta(t)$ and differentiated analytically to produce $\dot{\theta}(t)$ and, from Eq. 4, $\eta[\theta(t),\dot{\theta}(t)]$. The constant, k, in Eq. 4 could be estimated from particle twisting in viscosity standards to be 10.4 Pa. A parametric plot of η versus $\dot{\theta}$ was constructed, with a 95% confidence region derived from the statistics of the empirical fit to $\theta(t)$.

RESULTS

Microscopy

Observation of lung macrophages in culture chambers with a microscope verified that the cells harvested after animal aerosol exposure had ingested numerous magnetic particles. That the intracellular particles were magnetic and could rotate in response to changing magnetic field directions is illustrated for living cells in Fig. 1. Time-lapse videomicroscopy of the macrophages revealed cytoplasmic motions consisting of ruffling of the cell border as well as translocation and rotation of particle-containing intracellular organelles. These data confirmed that magnetic "relaxation" is correlated to cytoplasmic motion and that forced rotation of the particle/phagosome units is hindered by apparent cytoplasmic viscosity (Valberg, 1984; Valberg and Albertini, 1985).

Videomicroscopy and electron micrographs showed that before application of a strong permanent magnet (0.1 T), particle-containing phagosomes within cells were generally separate, spherical structures. Within 15 s of positioning the cells adjacent to the permanent magnet, phagosomes would elongate in the direction of the field lines, and previously separate phagosomes would link up into chains. This was apparent in electron micrographs of the intracellular particles. Lavaged cells collected at the bottom of a centrifuge tube were fixed either without magnetization or immediately after 2 min of magnetization using a Co-Sm permanent magnet that produced a field of ~170 mT through the cell pellet. Fig. 2 gives the ultrastructural appearance of γ-Fe_2O_3 particles within lung macrophages. Particle-containing vacuoles can be seen elongated and chained together in lines parallel to the applied field direction. Particles can be magnetized without these changes by alignment of particle magnetic moments via a brief pulse (< 10 μs) of an ~0.1 T magnetic field.

Model Fitting Data for Macrophages under Control Conditions

Fig. 3 illustrates how relaxation curve data for control cells fit the postulated mechanisms of particle/organelle motion. The experimental points are from an in vitro macrophage relaxation curve. The solid lines represent the best fit to the data, and dashed lines outline a 95% confidence band for the curve. In Fig. 3 *A* we fitted the Brownian motion model, Eq. 5 (two parameters), and it is clear that the data are not consistent with the single mechanism. In Fig. 3 *B*, the double-exponential model, Eq. 6 (four parameters), shows improved fit. In Fig. 3 *C*, the mechanism of internal reorientation via "linear-tracks," Eq. 8 (three parameters), also shows a good fit. The best result is shown in Fig. 3 *D*, where particles simultaneously undergo Brownian motion and internally driven motion along "linear tracks," Eq. 9 (four parameters). The result is a marked improvement over two exponentials and yet contains an equal number of parameters.

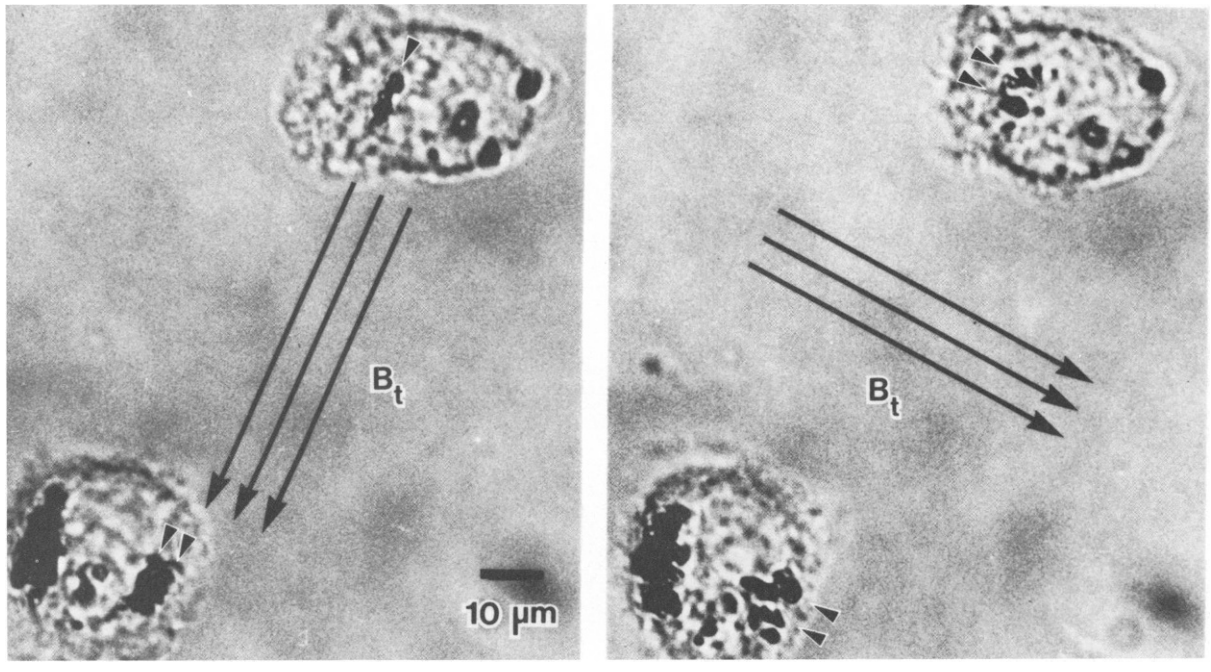

FIGURE 1 Micrographs of two lung macrophages and the magnetic responsiveness of γ-Fe_2O_3 particles within them. The direction of the applied magnetic field is shown (*arrows*), and the reorientation of the intracellular magnetic particles (*arrowheads*) to changes in field direction is visible.

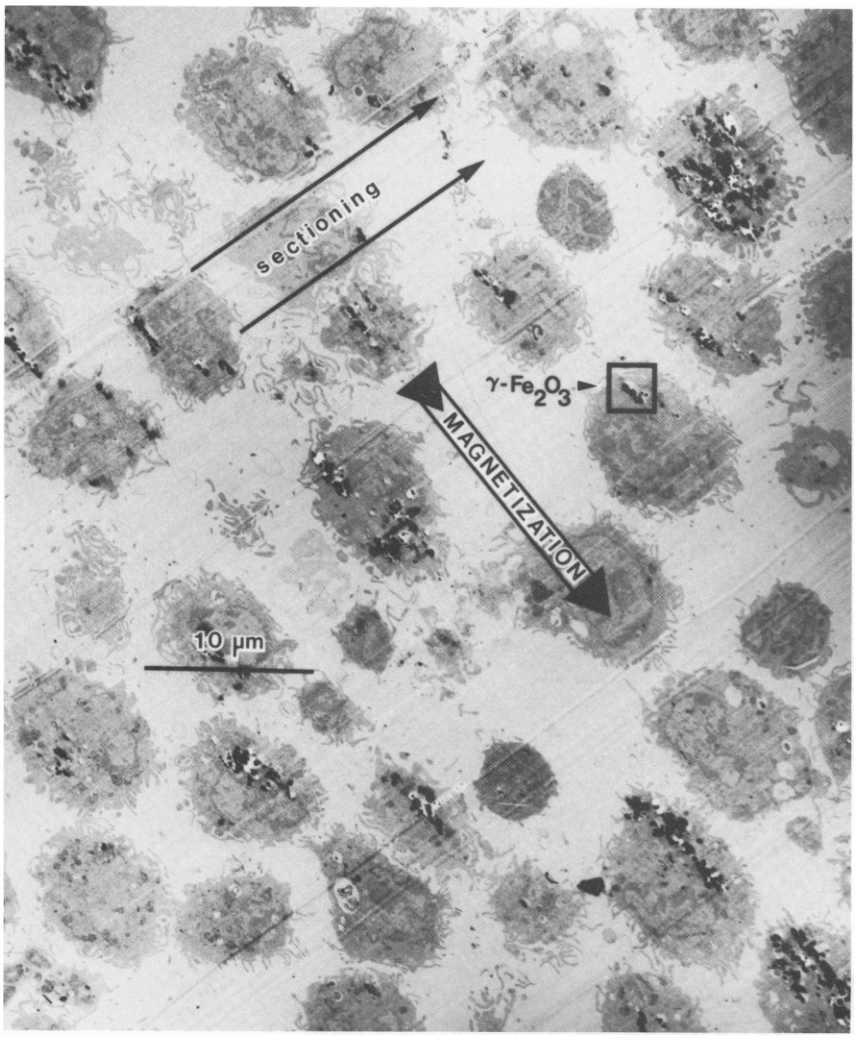

FIGURE 2 Transmission electron micrograph of macrophages fixed after a 2-min application of a permanent magnet. The magnetization field lines were in the plane of the section, as shown. Tissue blocks were sectioned at right angles to field lines to assure that particle chains were not produced by the cutting process.

Time Duration of Particle Magnetization

The effect of the duration of macrophage magnetization on subsequent relaxation was investigated over magnetization times ranging from a 10 μs pulse to 20 min. The changes in the shape of relaxation curves can be seen in Fig. 4 *A* (average of cells from four animals), where the curves are normalized to 100% at $t = 0$. These data were fitted to Eq. 9, and changes in the parameters with duration of magnetization are displayed in Fig. 4 *B*. The most rapid initial relaxation (expressed by the parameter α) was observed after the 0.2-min magnetization; this most likely reflects elastic energy storage in the cytoplasm. As the particles were held in the aligned position for longer periods of time (2 min and 20 min), this elastic energy apparently became dissipated, and relaxation slowed. The initially faster relaxation of the pulse-magnetization curve may have been due to the higher mobility of phagosomes that had not been linked together by the magnetization process. The magnitude of the initial remanent field increased with duration of magnetization. As can be seen in *B*, the relative magnitudes were: pulse, 0.50; 12 s, 0.81; 120 s, 0.94; 1,200 s, 1.00. This can be explained by the long axis of particles lining up with the applied field and particles linking up into linear arrays that have lower demagnetizing factors. This is consistent with the behavior of an initially randomly oriented array of monodomain particles.

Incubation of Cells with Cytochalasin D

CytD was dissolved in DMSO, and aliquots of cells were incubated for 15 min with cytD concentrations ranging from 0.03 to 10.0 μM (0.3% DMSO), or with 0.3% DMSO alone. CytD reduced the decay rate of the remanent field, as seen in Fig. 5. The "linear track pulling" model (Eq. 8) fit the experimental curves quite well even with the parameter β fixed at ½. The parameter α was sensitive to cytD concentration. We conclude that increasing concentrations of cytD progressively disrupted actin-filament function and inhibited magnetometrically measured cytoplasmic motility. These curves were examined closely using our nonlinear model-fitting procedure for the five separate models of remanent field decay (Eqs. 5–9). The "diffusing-rod" model of Doi and Edwards (1978) was included as yet another comparison to the "linear track" model. Doi and

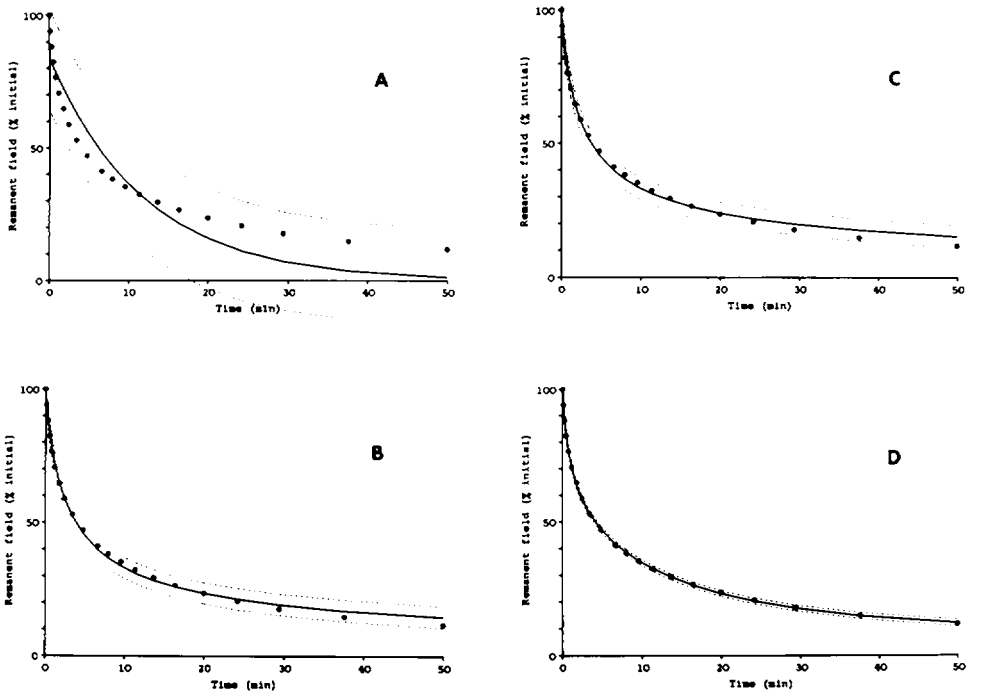

FIGURE 3 Relaxation data (*solid circles*) fitted to the predictions of various mechanisms of relaxation (*solid lines*). (*A*) Brownian rotation. (*B*) Double-exponential. (*C*) Linear-track pulling. (*D*) Simultaneous linear-track and Brownian rotation operating independently. Dashed lines enclosed the 95% confidence band. Not shown: rod-diffusion model.

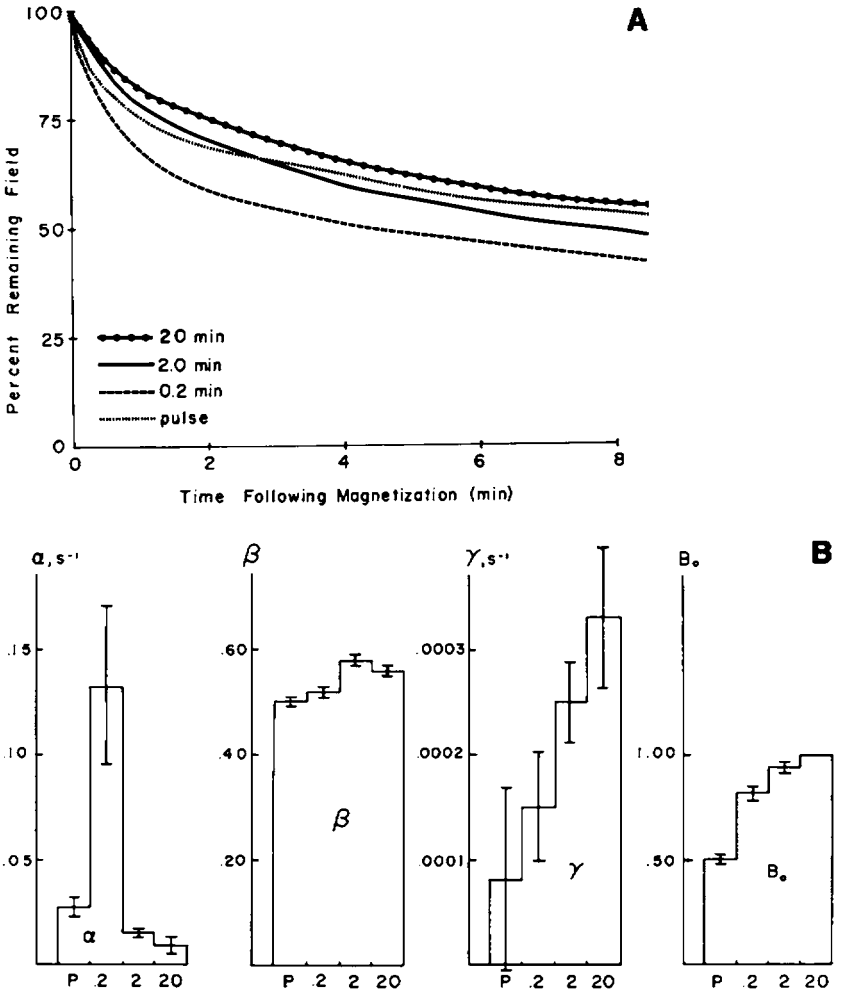

FIGURE 4 (*A*) Relaxation curves for lung macrophages in vitro measured immediately after magnetization durations as shown (pulse, 10 μs). (*B*) Changes in parameters fitted to the curves, assuming simultaneous linear-track pulling and Brownian rotation, Eq. 9. Magnetization duration is identified by its length in minutes except $P=10$ μs pulse.

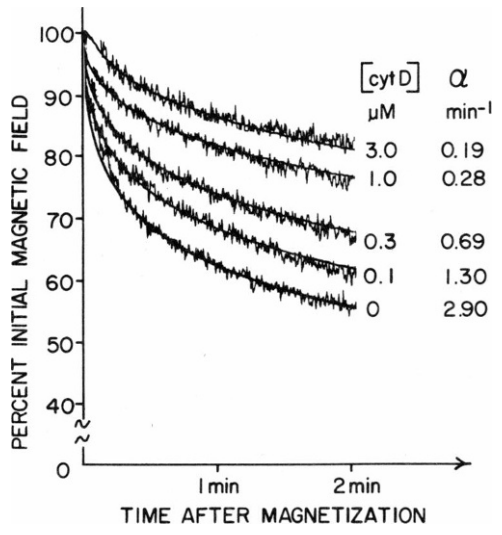

FIGURE 5 Relaxation curves and fitted parameters for macrophages incubated at 37°C and treated for 15 min with concentrations of cytD as shown. The data for remanent field 0–2 min are the noisy traces, and the solid line shows the fitted curve corresponding to the value of the parameter α as given to the right of the curve (Eq. 8 with $\beta = \frac{1}{2}$).

Edwards showed that rotary Brownian diffusion of rod-like objects in nonexponential, and if our magnetic particles were adherent to long intracellular filaments, it could be argued that this result ought to apply to them. As can be seen in Table I, the residual mean square error of the single exponential (Brownian) mechanism was very high. The linear-track model provided the best fit and had parameters (α and β) that were responsive to cytD concentration. Adding a Brownian term gave only a slight improvement in this case. The rod-diffusion model did better than the single exponential, but not as well as linear tracks, and furthermore, it required a nonphysical exponentially increasing term (γ) for good fit.

Twisting of Intracellular Particles with an External Field

Analysis of particle rotation produced by external fields can gauge the apparent viscous environment. Direct tracings of the recorded cell magnetometer output are given in Fig. 6. The upper curve is the remanent magnetic field decay due to spontaneous cytoplasmic motility within living lung macrophages containing magnetic particles. The magnitude of the field decays to 39% of its initial value in 5 min. The lower curve in Fig. 6 is the time course of the remanent field for the same cells during continuous application of the 2.5 mT twisting field acting to rotate intracellular particles away from their original direction of magnetization. Under twisting, the field decays to 12% of its inital value in 5 min. The quotient of $B_{r,notwist}(t)$ and $B_{r,twist}(t)$ was used as described (Eqs. 3 and 4) to generate a plot of $\eta(\dot{\theta})$ versus $\dot{\theta}$ both for control cells and for cytD-treated cells. The apparent viscosity in the 0–20-s interval, at higher shear rates (0.05 s^{-1}), was 254 Pa-s. In the 20–100-s interval, when shear was lower (0.001 s^{-1}), apparent viscosity was 2745 Pa-s. Fig. 7 shows a plot of $\eta(\dot{\theta})$ versus $\dot{\theta}$. The marked shear-dependence of η indicates that the cytoplasm is distinctively non-Newtonian. It can also be seen that the shear dependence of η was similar for cytD-treated cells and for control cells, being only slightly steeper for control cells than for cytD-treated cells. That is,

TABLE I
FITTED MODELS FOR RELAXATION CURVES

Model	Parameters	RPMI 1640 control 1	RPMI 1640 control 2	DMSO 0.3%	CytD 0.03 μM	CytD 3.0 μM	CytD 10.0 μM
		Residual mean square error × 10^4 =					
Brownian, Eq. 5	2	288.6	396.1	610.3	729.0	184.0	117.5
Biexponential, Eq. 6	4	5.7	8.7	18.0	20.7	18.0	5.6
Rod diffusion, Eq. 7	3	1.9	5.8	5.1	12.0	18.3	7.2
Linear tracks, Eq. 8	3	1.5	3.2	2.7	5.0	9.4	6.0
Brownian + linear tracks, Eq. 9	4	1.3	3.2	2.8	5.1	—*	5.3
				Fitted values			
Brownian	$\gamma(s^{-1})$	0.0020	0.0024	0.0018	0.0019	0.0008	0.0004
Biexponential	$\gamma_1(s^{-1})$	0.0369	0.0467	0.0390	0.0452	0.0778	0.0462
	$\gamma_2(s^{-1})$	0.0011	0.0013	0.0010	0.0011	0.0006	0.0002
	f	0.260	0.307	0.243	0.260	0.196	0.091
Rod diffusion	$\lambda(s^{-1})$	0.00338	0.00561	0.00300	0.00371	0.00060	0.00034
	$\gamma(s^{-1})$	−0.00112	−0.00167	−0.00109	−0.00135	−0.00050	−0.00050
Linear tracks	$\alpha(s^{-1})$	0.0210	0.0415	0.0199	0.0295	0.0029	0.0006
	β	0.574	0.570	0.536	0.504	0.336	0.216
Brownian + linear tracks	$\alpha(s^{-1})$	0.0204	0.0400	0.0199	0.0298	—*	0.0008
	β	0.610	0.586	0.538	0.502	—	0.332
	$\gamma(s^{-1})$	0.00011	0.00005	0.00000	0.00001	—	0.00011

*Model-fitting procedure failed to converge.

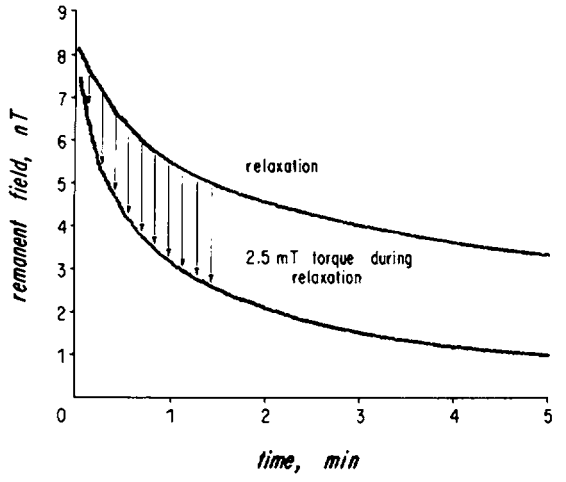

FIGURE 6 Remanent-field decay from viable γ-Fe_2O_3-containing lung macrophages in vitro in the absence (*upper curve*) and presence (*lower curve*) of the twisting field. The contribution from twisting per se is represented by the vertical distance between the two curves, as shown by the arrows.

control cells had a lower apparent viscosity at high shear rates (>0.03 s^{-1}) and a higher apparent viscosity at low shear rates (<0.0003 s^{-1}).

DISCUSSION

Measurements of Cell Motions

The functional capabilities of cells in the body can be broadly classified into chemical synthesis (secretion) and physical movement (contraction). Although gland cells and muscle cells are highly specialized, respectively, in secretion and contraction, all cells possess these functions to variable degrees. There exist well established methods for examining chemical synthesis by cells (e.g., histochemistry, protein chromatography and electrophoresis, precursor radiolabeling, and radioimmunoassay). On the other hand, cytoplasmic motions in non-muscle cells have been measured by just one technique: optical observation. The term "cell motility" encompasses the motions of the cytoplasm as seen in a variety of cell activities, such as vesicle translocation, membrane ruffling, phagocytosis, phagolysosome fusion, cell reorientation, and cell translocation. Although there may exist a common "motor" that drives all of these activities in a given cell, it is also true that different systems have been described for moving intracellular organelles: actin–myosin interactions (Sheetz and Spudich, 1983; Euteneuer and Schliwa, 1985; Adams and Pollard, 1986) or microtubule–organelle interactions (Beckerle, 1984; Hayden et al., 1983; Vale et al., 1985). Even so, cytoplasmic motion in non-muscle cells is poorly understood; yet, important cell functions such as chemotaxis and phagocytosis rely on the generation of intracellular motion.

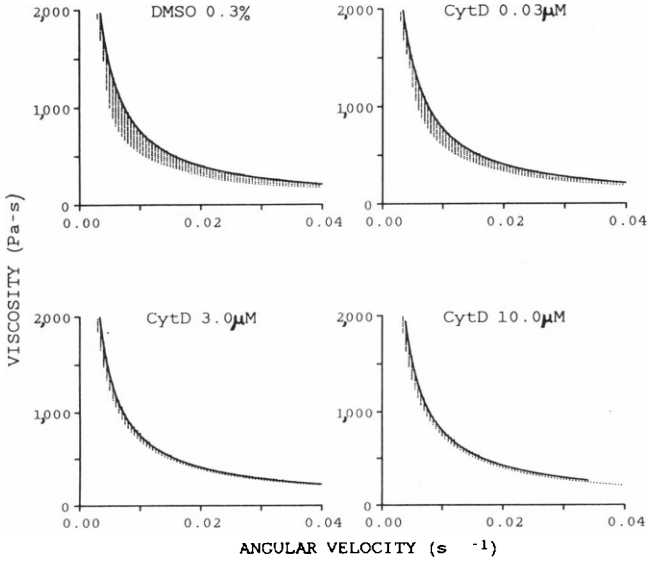

FIGURE 7 Plot of apparent viscosity versus shear rate for control cells and cells incubated with three different concentrations of cytD. Shading indicates the 95% confidence region for the curve. Asymmetry of the confidence region is due to correlated uncertainty in the values of η and θ.

We have described an alternative to optical microscopy for quantifying organelle mobility which uses intracellular magnetic particles whose remanent field can be detected with a sensitive magnetometer. To the extent that magnetic particle–containing organelles are moved and rotated as a result of any motile activities, the magnetometric method will sense this. For example, intracellular fluorescent microspheres have been successfully used to monitor cytoplasmic motions (Beckerle, 1984), and submicron magnetic particles can be used in a similar way with the following advantages. (*a*) Preparation of cells on the stage of a microscope, optical observation, and morphometric analysis are not necessary. (*b*) The particles can be made to exert a known force on their environment and thus probe resistance to movement and elasticity. (The forces resisting organelle movement are important to know since the rate of phagocytosis, movement, activation, exocytosis in cells may be limited by cell viscosity.) (*c*) The procedures and interpretations developed during studies of cells in vitro can be applied via the same technique to cells in situ within the body.

Magnetometric signals from isolated lung macrophages have been correlated to the effects of metabolic inhibitors and cytoskeletal poisons (Valberg, 1984; Valberg and Albertini, 1985; Gehr et al., 1985; Nemoto et al., 1985; Toyotama and Nemoto, 1985), demonstrating that the relaxation phenomenon is associated with motions of the macrophage cytoplasm. The stage is now set for the application of magnetometry as a tool for measurement of cell function and for manipulation and modification of cell function by magnetic particles within cells in vitro. Moreover, there exist data on relaxation in lungs of intact animals and humans (Valberg and Brain, 1979; Gehr et al., 1983; Brain et al., 1984; Cohen et al., 1984), the

interpretation of which will be aided by correlation with in vitro data for magnetite-containing cells under controlled conditions. For example, the clearance of magnetic material from lungs or other organs can be followed by repetitive determination of B_0, the remanent field before relaxation. Since B_0 is obtained by extrapolation of the relaxation curve back to $t = 0$ (the instant at which magnetization ends), an accurate mathematical model for relaxation is required. Our cell studies suggest that the "linear tracks" equation may be more suitable for modeling relaxation in vivo than a single decaying exponential.

Measurements of Cell Viscosity

Cytoplasmic viscosity is likely important to many cellular processes, and cells might be expected to exhibit considerable diversity in internal viscosity based on the size of the particle being observed, the shear rate, and the amount of internal membrane and filamentous structure typical of that cell type. One of the early analytical studies of living cytoplasm was published by Crick and Hughes (1950), who used small particles of oxidized iron which were moved about magnetically and whose motions were followed optically. The viscosity studies of Crick and Hughes and others (Table II) have generally used either large particles (~100 μm) or molecular probes of small size (~0.003 μm). The larger particles have been observed optically, and the molecules have been monitored by techniques that measure their diffusion mobility.

The magnetometric approach has provided new data in several respects. First, most of the work on cytoplasmic viscosity has been done in invertebrate cells (Rubinson and Baker, 1979; MacLean-Fletcher and Pollard, 1980*b*; Sato et al., 1984; Salmon et al., 1984), which may have different viscoelastic properties than mammalian cells. We used mammalian macrophages, and important functions of these cells such as phagocytosis and cell movement are likely influenced by cytoplasmic viscosity. Second, most studies in mammalian cells have involved either viscosity on a molecular scale (Wojcieszyn et al., 1981; Wange et al., 1982; Mastro et al., 1984), or whole-cell deformation measured in rheometers or by micropipette aspiration (Sung et al., 1982; Cranston et al., 1984; Evans and Kukan, 1984). Yet, measured cell viscosity is dramatically determined by the size of the probe (see Table II). The particles we used are similar in size to cell organelles (~0.5 μm) and experience markedly different apparent viscosity than molecules. We suggest that magnetic particles in phagosomes more accurately probe the resistance that needs to be overcome in vesicle motion than do probes that are much larger or much smaller. Third, large magnetic spheres within cells have generally been pulled (which may disrupt cytoplasm) and their motion recorded photgraphi-

TABLE II
EXPERIMENTAL MEASUREMENTS OF CYTOPLASMIC VISCOSITY

Investigators, date	Experimental parameters				
	Cell system	Method	Particle diameter	Shear rate	Apparent viscosity
			μm	s^{-1}	*Pa-s*
Crick and Hughes, 1950	Chick fibroblasts	Magnetic dragging, optical analysis	2–5	1.4	~1
Yagi, 1961	Ameba	Magnetic dragging, optical analysis	2–9	3.0	0.01–0.30
Hiramoto, 1969	Sea urchin egg	Magnetic dragging, optical analysis	5–9	0.5–2.0	~10
Maruyama et al, 1974	F-actin 0.003 mg/ml	Rotational viscometer	(d = 1 cm)	0.0005	44
Rubinson and Baker, 1979	Squid axon	Capillary, plug flow	(id = 500)	0.2–1.0	14.6
MacLean-Fletcher and Pollard, 1980*a*, *b*	Actin, sol-gel	Falling ball viscometer	640	0–10	Sol = 0.002 Gel > 12
Wojcieszyn et al., 1981	Foreskin fibroblasts	FPR, BSA	0.0072	na	0.08
Nemoto, 1982	Particles in lungs	Response to magnetization	1.3	0.005	320–480
Sung et al., 1982	Human neutrophils	Micropipette aspiration	(id = 3)	0.01–0.02	~10
Wang et al., 1982	Ameba	FPR, BSA	0.0072	na	0.001–0.002
Sato et al., 1983	Physarium	Magnetic dragging, optical analysis	4–16	0.5–3.0	0.1–0.5
Sato et al., 1984	Squid axoplasm	Magnetic dragging, optical analysis	83–213	0.0001–0.004	10^4–10^5
Salmon et al., 1984	Sea urchin egg	FPR, BSA	0.0072	na	0.006
Mastro et al., 1984	Swiss 3T3 cells	ESR, PCAOL	0.00064	na	0.002–0.003
Valberg and Albertini, 1985	Pulmonary macrophages	Magnetometry of twisted particles	0.3–0.7	0.001–0.003	1,200–2,700
Luby-Phelps et al., 1986	Swiss 3T3 cells	FPR, dextran	0.0012	na	0.004

Viscosity of H_2O = 0.0007 Pa-s at 37°C. FPR, fluorescence photobleaching recovery; ESR, electron spin resonance; PCAOL, tetramethylmethanolpyrroline-*N*-oxyl. na, not applicable, molecular diffusion does not have a defined shear rate. id, inner diameter.

cally (Yagi, 1961; Sato et al., 1984). In the magnetometric method, particles are twisted while in one area of the cell. No translocation across intracytoplasmic barriers is required. The magnetic-particle method is also sensitive to cytoplasmic elastic properties, which are not measurable by molecular-diffusion techniques. Fourth, the magnetometric method can be used in vivo. This has been done by Nemoto (1982), who examined the magnetization curves of lung-retained particles and estimated the apparent viscosity to be in the range 320–480 Pa-s at shear rates of $0.005\ s^{-1}$. It should be kept in mind, however, that viscosity parameters for non-Newtonian systems should not be taken too literally. As was discussed in the previous paper (Valberg and Butler, 1987), the non-Newtonian nature of the cytosol, the possible existence of links to filamentous elements, and the unknown viscosity differences between the cytosol and the phagosome interior all make identification of the locale at which fluid shear takes place in intact cells difficult and assignment of an absolute viscosity value impossible. Nonetheless, the twisting of intracellular particles can provide parameters by which to express the resistance to driven rotation, an apparent viscosity.

The role of cytoskeletal proteins in cell rheology has also been investigated (MacLean-Fletcher and Pollard, 1980*b*; Zaner and Stossel, 1982). A recent study of both f-actin and microtubule suspensions in a rheogoniometer reported viscosity inversely proportional to shear rate, much like the data we give in Fig. 7 (Buxbaum et al., 1987). Stabilization and disruption of the cytoskeleton can be accomplished within intact cells (e.g., Brown and Spudich, 1981; Albertini et al., 1984; Cassimeris et al., 1986), yet data on how such alterations affect cytoplasmic consistency (viscosity, elasticity) are lacking. Furthermore, cytoplasmic viscosity changes consequent to changes in cell function are yet to be determined. Recent physical models of cell motion (Dembo and Harlow, 1986) are hampered by inadequate viscometric data on intact mammalian cytoplasm.

SUMMARY

In conclusion, magnetometric analysis of particle/organelle motions can be applied to cells both in vitro and in vivo, and new information is provided by this intracellular probe system. Magnetometric data may eventually aid in noninvasive assessment of normal cell function or cell pathology within human subjects.

The authors thank D. F. Albertini, N. R. Bertram, S. B. Bloom, J. D. Brain, D. Cohen, and B. Herman for help and advice.

This work was supported by National Institutes of Health grants CA-40696, ES-00002, and HL-31029.

Received for publication 2 February 1987 and in final form 4 May 1987.

REFERENCES

Adams, R. J., and T. D. Pollard. 1986. Propulsion of organelles isolated from *Acanthamoeba* along actin filaments by myosin-I. *Nature (Lond.)*. 322:754–756.

Albertini, D. F., B. Herman, and P. Sherline. 1984. *In vivo* and *in vitro* studies on the role of HMW-MAPs in taxol-induced microtubule bundling. *Eur. J. Cell Biol.* 33:134–143.

Beckerle, M. C. 1984. Microinjected fluorescent polystyrene beads exhibit saltatory motion in tissue culture cells. *J. Cell Biol.* (98:2126–2132.

Brain, J. D., S. B. Bloom, P. A. Valberg, and P. Gehr. 1984. Correlation between the behavior of magnetic iron oxide particles in the lungs of rabbits and phagocytosis. *Exp. Lung Res.* 6:115–131.

Brain, J. D., and N. R. Frank. 1968. Recovery of free cells from rat lungs by repeated washings. *J. Appl. Physiol.* 25:63–69.

Brown, S. S., and J. A. Spudich. 1981. Mechanism of action of cytochalasin: evidence that it binds to actin filament ends. *J. Cell Biol.* 88:487–491.

Buxbaum, R. E., T. Dennerll, S. Weiss, and S. R. Heidemann. 1987. F-actin and microtubule suspensions as indeterminate fluids. *Science (Wash. DC)*. 235:1511–1514.

Cassimeris, L. U., P. Wadsworth, and E. D. Salmon. 1986. Dynamics of microtubule depolymerization in monocytes. *J. Cell Biol.* 102:2023–2032.

Chandler, D. B., W. C. Fuller, R. M. Jackson, and J. D. Fulmer. 1986. Fractionation of rat alveolar macrophages by isopycnic centrifugation: morphological, cytochemical, biochemical, and functional properties. *J. Leukocyte Biol.* 39:371–383.

Cohen, D. 1973. Ferromagnetic contaminants in the lungs and other organs of the body. *Science (Wash. DC)*. 180:745–748.

Cohen, D. 1978. Report of the Low-Field Group: The Magnetic Field of the Lung. Publication MIT/FBNML-78/1. Nat. Tech. Inform. Service, Springfield, VA.

Cohen, D., and I. Nemoto. 1984. Ferrimagnetic particles in the lung. Part I: the magnetizing process. *IEEE (Inst. Electr. Electron. Eng.) Trans. Biomed. Eng.* BME-31:261–273.

Cohen, D., I. Nemoto, L. Kaufman, and S. Arai. 1984. Ferrimagnetic particles in the lung. Part II: the relaxation process. *IEEE (Inst. Electr. Electron. Eng.) Trans. Biomed. Eng.* BME-31:274–285.

Cranston, H. A., C. W. Boyland, G. L. Carroll, S. P. Sutera, J. R. Williamson, I. Y. Gluzman, and D. J. Krogstad. 1984. *Plasmodium falciparum* maturation abolishes physiologic red cell deformability. *Science (Wash. DC)*. 223:400–403.

Crick, F. H. C., and A. F. W. Hughes. 1950. The physical properties of cytoplasm: a study by means of the magnetic particle method. *Exp. Cell Res.* 1:37–80.

Dembo, M., and F. Harlow. 1986. Cell motion, contractile networks, and the physics of interpenetrating reactive flow. *Biophys. J.* 50:109–122.

Doi, M., and S. F. Edwards. 1978. Dynamics of rod-like macromolecules in concentrated solution, Part 1. *J. Chem. Soc Faraday Trans. II.* 74:560–570.

Euteneuer, U., and M. Schliwa. 1985. Evidence for an involvement of actin in the positioning and motility of centrosomes. *J. Cell Biol.* 101:96–103.

Evans, E., and B. Kukan. 1984. Passive material behavior of granulocytes based on large scale deformation and recovery after deformation tests. *Blood.* 64:1028–1035.

Gehr, P., J. D. Brain, I. Nemoto, and S. B. Bloom. 1983. Behavior of magnetic particles in hamster lungs: estimates of clearance and cytoplasmic motility. *J. Appl. Physiol. Respir. Environ. Exercise Physiol.* 55:1196–1202.

Gehr, P., J. D. Brain, I. Nemoto, and S. B. Bloom. 1985. Organelle movements of alveolar macrophages studied by cytomagnetometry. *In* Biomagnetism: Applications and Theory. H. Weinberg, G. Stroink, and T. Katila, editors. Pergamon Press, New York. 395–400.

Gibb, F. R., and P. E. Morrow. 1962. Alveolar clearance in dogs after inhalation of an iron 59 oxide aerosol. *J. Appl. Physiol.* 17:329–432.

Grant, M., S. Sorokin, and J. Brain. 1979. Lysosomal enzyme activities in pulmonary macrophages from rabbits breathing iron oxide. *Am. Rev. Respir. Dis.* 120:1003–1012.

Hayden, J. H., R. D. Allen, and R. D. Goldman. 1983. Cytoplasmic transport in keratocytes: direct visualization of particle transport along microtubules. *Cell Motil.* 3:1–19.

Hiramoto, O. 1969. Mechanical properties of the protoplasm of the sea urchin egg. *Exp. Cell Res.* 56:201–208.

Jennrich, R. I., and M. L. Ralston. 1979. Fitting nonlinear models to data. *Annu. Rev. Biophys. Bioeng.* 8:195–238.

Kavet, R. I., and J. D. Brain. 1980. Methods to quantify endocytosis: a review. *J. Reticuloendothel. Soc.* 27:201–221.

Kavet, R. I., J. D. Brain, and D. J. Levens. 1978. Characteristics of pulmonary macrophages lavaged from hamsters exposed to iron oxide aerosols. *Lab. Invest.* 38:312–319.

Kronick, P. L. 1980. Magnetic microspheres in cell separation. *Methods Cell Sep.* 3:115–139.

Luby-Phelps, K., K. D. Taylor, and F. Lanni. 1986. Probing the structure of cytoplasm. *J. Cell Biol.* 102:2015–2022.

MacLean-Fletcher, S., and T. D. Pollard. 1980*a*. Mechanism of action of cytochalasin B on actin. *Cell.* 20:329–341.

MacLean-Fletcher, S., and T. D. Pollard. 1980*b*. Viscometric analysis of the gelation of *Acanthamoeba* extracts and purification of two gelation factors. *J. Cell Biol.* 85:414–428.

Maruyama, O., M. Kaibara, and E. Fukada. 1974. Rheology of F-actin: I. Network of F-actin in solution. *Biochim. Biophys. Acta.* 371:20–29.

Mastro, A. M., M. A. Babich, W. D. Taylor, and A. D. Keith. 1984. Diffusion of a small molecule in the cytoplasm of mammalian cells. *Proc. Natl. Acad. Sci. USA.* 81:3414–3418.

Nemoto, I., H. Toyotama, P. Gehr, and J. D. Brain. 1985. *In vivo* and *in vitro* measurements of magnetic relaxation in hamster pulmonary macrophages. *In* Biomagnetism: Applications and Theory. H. Weinberg, G. Stroink, and T. Katila, editors. Pergamon Press, New York. 433–437.

Nemoto, I. 1982. A model of magnetization and relaxation of ferrimagnetic particles in the lung. *IEEE (Inst. Electr. Electron. Eng.) Trans. Biomed. Eng.* BME-29:745–752.

Parod, R. J., and J. D. Brain. 1986. Immune opsonin-independent phagocytosis by pulmonary macrophages. *J. Immunol.* 136:2041–2047.

Porter, K. R. 1984. Cytoskeleton symposium: cytoplasmic matrix and the integration of cellular function. *J. Cell Biol.* 99(1,Pt.2):1s–248s.

Reppun, T. S., H. S. Lin, and C. Kuhn. 1979. Isokinetic separation and characterization of mouse pulmonary alveolar colony-forming cells. *J. Reticulendothel. Soc.* 25:379–387.

Rubinson, K. A. and P. F. Baker. 1979. The flow properties of axoplasm in a defined chemical environment: influence of anions and calcium. *Proc. R. Soc. Lond. B. Biol. Sci.* 205:323–345.

Salmon, E. D., W. M. Saxton, R. J. Leslie, M. L. Karow, and J. R. McIntosh. 1984. Diffusion coefficient of fluorescein-labeled tubulin in the cytoplasm of embryonic cells of a sea urchin: video image analysis of fluorescence redistribution after photobleaching. *J. Cell Biol.* 99:2157–2164.

Sato, M., T. Z. Wong, and R. D. Allen. 1983. Rheological properties of living cytoplasm: endoplasm of *Physarium* plasmodium. *J. Cell Biol.* 97:1089–1097.

Sato, M., T. Z. Wong, D. T. Brown, and R. D. Allen. 1984. Rheological properties of living cytoplasm: a preliminary investigation of squid axoplasm (Loligo pealei). *Cell Motil.* 4:7–23.

Sheetz, M. P., and J. A. Spudich. 1983. Movement of myosin-coated fluorescent beads on actin cables in vitro. *Nature (Lond.).* 303:31–35.

Sorokin, S. P., and J. D. Brain. 1975. Pathways of clearance in mouse lungs exposed to iron oxide aerosols. *Anat. Rec.* 181:581–626.

Sung, K. P., W. Schmid-Schönbein, R. Skalak, B. Schuessler, U. Shunichi, and S. Chien. 1982. Influence of physicochemical factors on rheology of human neutrophils. *Biophys. J.* 39:101–106.

Toyotama, H., and I. Nemoto. 1985. Measurements of the behavior of magnetic fine particles in a macrophage-like cell line (J774.1). *In* Biomagnetism: Applications and Theory. H. Weinberg, G. Stroink, and T. Katila, editors. Pergamon Press, New York. 401–405.

Valberg, P. A. 1984. Magnetometry of ingested particles in pulmonary macrophages. *Science (Wash. DC).* 224:513–516.

Valberg, P. A., and D. F. Albertini. 1985. Cytoplasmic motions, rheology, and structure probed by a novel magnetic particle method. *J. Cell Biol.* 101:130–140.

Valberg, P. A., and J. D Brain. 1979. Generation and use of three types of iron-oxide aerosol. *Am. Rev. Respir. Dis.* 120:1013–1024.

Valberg, P. A., and J. P. Butler. 1987. Magnetic particle motions within living cells: physical theory and techniques. *Biophys. J.* 52:537–550.

Valberg, P. A., and E. Mariak. 1984. Magnetic separation of lung macrophages by phagocytic ability. *Fed. Proc.* 43:700. (Abstr.)

Vale, R. D., B. J. Schnapp, T. S. Reese, and M. P. Sheetz. 1985. Movement of organelles along filaments dissociated from the axoplasm of the giant squid axon. *Cell.* 40:449–454.

Wang, Y.-L., F. Lanni, P. L. McNeil, B. R. Ware and D. L. Taylor. 1982. Mobility of cytoplasmic and membrane-associated actin in living cells. *Proc. Natl. Acad. Sci. USA.* 79:4660–4664.

Wojcieszyn, J. W., R. A. Schlegel, E. S. Wu, and K. A. Jacobson. 1981. Diffusion of injected macromolecules within the cytoplasm of living cells. *Proc. Natl. Acad. Sci. USA.* 78:4407–4410.

Yagi, K. 1961. The mechanical and colloidal properties of *Amoeba* protoplasm and their relations to the mechanism of amoeboid movement. *Exp. Biochem. Physiol.* 3:73–91.

Zaner, K. S., and T. P. Stossel. 1982. Some perspectives on the viscosity of actin filaments. *J. Cell Biol.* 93:987–991.